Macromolecules

Article

pubs.acs.org/Macromolecules

Cobaltoporphyrin-Catalyzed CO_2/Epoxide Copolymerization: Selectivity Control by Molecular Design

Carly E. Anderson, Sergei I. Vagin, Wei Xia, Hanpeng Jin, and Bernhard Rieger*

WACKER-Chair for Macromolecular Chemistry, Technical University of Munich, Lichtenbergstrasse 4, D-85748 Garching bei Munich, Germany

Supporting Information

ABSTRACT: A series of cobalt(III) chloride porphyrin complexes of the general formula 5,10,15,20-tetra(*p*-alkoxy)-phenylporphyrin cobalt chloride (**4b−e**) and the related 5,10,15,20-tetra(*p*-nitro)phenylporphyrin cobalt chloride (**4f**) are presented and their reactivity toward propylene oxide (PO)/CO_2 coupling/copolymerization is explored. While the nitro-substituted complex (**4f**), in conjunction with an onium salt, shows moderate activity toward cyclization, the **4b−e**/onium systems show superior copolymerization activity in comparison to tetraphenylporphyrin Co(III) chloride (**4a**) with high selectivity and conversion to poly(propylene carbonate) (PPC). A comprehensive copolymerization behavior study of the alkoxy-substituted porphyrin complexes **4b−e** in terms of reaction temperature and CO_2 pressure is presented. Complexes bearing longer alkoxy-substituents demonstrate the highest polymerization activity and molecular weights, however all substituted catalyst systems display a reduced tolerance to increased temperature with respect to PPC formation. Studies of the resulting polymer microstructures show excellent head-to-tail epoxide incorporation and near perfectly alternating poly(carbonate) character at lower polymerization temperatures.

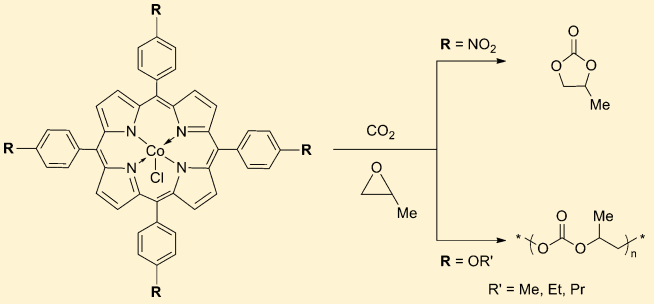

INTRODUCTION

Carbon dioxide is increasingly viewed as an attractive, low-cost C_1 carbon source for chemical processes due to its nontoxic, nonflammable, and abundant nature. The widespread application of carbon dioxide as a synthetic building block has traditionally been limited by its stable, relatively unreactive nature; however, major advances have been achieved in recent years with the activation/usage of CO_2 in transition metal-mediated reactions.[1,2] Foremost among these processes is the use of carbon dioxide as a comonomer for the production of aliphatic and aromatic poly(carbonates) in which CO_2 has the potential to replace the highly toxic phosgene in the synthesis of these industrially important polymers.[3−6]

Although a variety of monomers can be employed in CO_2/epoxide copolymerizations, copolymers comprising aliphatic epoxides are particularly attractive from an industrial viewpoint due to their excellent physical properties[7,8] and biodegradability.[9] Specifically poly(propylene carbonate) (PPC) is of interest due to its outstanding optical and mechanical properties such as high UV stability, transparency and Young's modulus, which make it ideal for applications in the automotive, food, and healthcare sectors. Consequently catalysts that are capable of copolymerizing propylene oxide (PO) and CO_2 to produce high molecular weight PPC are highly sought. Since the initial reports by Inoue and co-workers on active metalloporphyrin systems for the synthesis of poly(carbonates) with well-controlled molecular weight[10,11] there has been a drive toward the development of catalysts with ever increasing activities. To date, there remains a reliance on heterogeneous Zn-based dicarboxylate systems for the production of poly(carbonates) due to their ease of handling, low toxicity and economic viability.[12,13] However the active sites of these compounds are often poorly defined and their insoluble nature limits study of reaction mechanisms.[14,15] It is for these reasons that the development of coordination complexes that comprise well-defined active sites and high selectivity/activities for poly(carbonate) formation is an ongoing area of research.

In terms of homogeneous systems suitable for poly(carbonate) synthesis there exist a variety of complex systems capable of CO_2/epoxide copolymerizations.[3,6] Among these, metalloporphyrins are currently subject to a resurgence of interest which can be attributed to their facile synthesis and ease of handling. The unusually high reactivity of the porphyrin axial M−X bond[16] and their well-defined coordination modes with metal ions[17] make them attractive targets for catalyst development. Many previous studies have focused on aluminum-based porphyrin systems, however these typically suffer from lower activities (in comparison to other homogeneous systems) and an increased tendency for the resulting poly(carbonates) to contain significant amounts of

Received: June 14, 2012
Revised: August 3, 2012
Published: August 21, 2012

poly(ether) linkages[18] which negatively impact on the resulting polymer properties.[19]

The realization that cobalt-based complexes with various ligand types are able to catalyze epoxide/CO_2 coupling and copolymerization processes with high activities has led to a large number of reports in this area.[20] Furthermore, catalyst systems that selectively form poly(carbonates) over the coupled cyclic carbonate are favored as formation of the thermodynamically stable cyclic carbonate (CC) by a "backbiting" mechanism[21,22] is a major limitation and its suppression is desirable. Cobaltoporphyrins are advantageous in this respect as the catalyst selectivity toward copolymerization/coupling depends strongly on the nature of the employed cocatalyst[23] which ranges from selective cyclization[24,25] to production of high molecular weight poly(carbonate)[23,26] in accordance with variation of reaction parameters. The employed cocatalyst performs two principle roles in the polymerization reaction, namely labilizing the axial metalloporphyrin M−X bond (Chart 1), thereby "tuning" the electronic properties of the central metal,[18] and assisting PPC chain growth by promoting CO_2 insertion into the M−OR bond of a growing polymer chain.[6]

Chart 1. General M(III) Metalloporphyrin Structure, Showing Substitution (R_n) at the *meso*-Aryl Rings, Central Metal M and Axial Ligand X

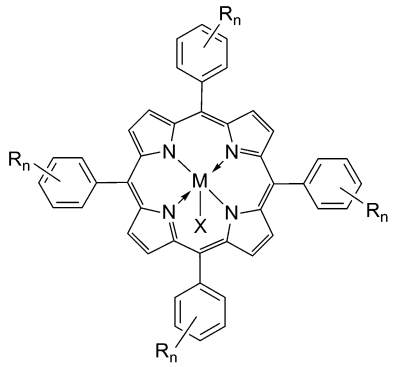

Another commonly used method of varying the coordination environment at the metal center is the concept molecular design by introduction of specific ligand fragments that influence the steric and electronic environment of the central metal ion. The planar, symmetrical nature of the porphyrin ring lends itself well to functionalization and this approach is increasingly used to modulate the complex reactivity and the resulting copolymerization behavior.[27,28] Indeed, it has been demonstrated that the judicious placement of electronically differing aryl-functionalities in the *meso*-position of the porphyrin framework raises the activity of the corresponding complexes toward ring-opening polymerization.[29]

To this end, a series of porphyrins bearing various alkoxy-functionalized aryl substituents in the *meso*-ring position have been developed and the reactivity of their respective cobalt complexes explored toward PO/CO_2 copolymerization reactions. As observed by Wang and co-workers, the placement of functionalities in the *ortho*-position of the *meso*-ring may interfere with monomer approach to the metal site,[25] and thus cobaltoporphyrins comprising substituents in the *para*-position were employed in these studies. Here we report a full study of effects of reaction conditions, specifically temperature and pressure, on the activity and selectivity of these complexes, in the presence of an onium cocatalyst, toward the copolymerization of propylene oxide and carbon dioxide and study of the obtained PPC.

EXPERIMENTAL SECTION

Methods and Materials. All reactions were routinely carried out under argon atmosphere using standard Schlenk techniques unless otherwise stated. Chemicals were obtained from Aldrich, ABCR, or Acros and used as received without further purification unless otherwise stated. Pyrrole (Acros Organics, 99% extra pure) and propylene oxide were purified by distillation from CaH_2 and stored under Ar atmosphere prior to use. Bis(triphenylphosphoranylidene) ammonium chloride (PPNCl) was purchased from Aldrich and stored under Ar atmosphere.

Solution NMR spectra were collected at ambient probe temperatures using a Bruker ARX300 or AV500 spectrometer. ^{1}H and ^{13}C{^{1}H} NMR spectra were referenced to residual protio impurities in the solvent (^{1}H) or the ^{13}C shift of the solvent (^{13}C). Solvent proton shifts (ppm): $CDCl_3$, 7.26 (s); DMSO-d_6, 2.50 (s). Solvent carbon shifts (ppm): $CDCl_3$, 77.2 (t); DMSO-d_6, 39.5 (sept). ^{13}C NMR spectra were assigned with the aid of DEPT 90, DEPT 135 and ^{1}H−^{13}C correlation experiments. Chemical shifts are reported in ppm and coupling constants in Hz. Mass spectrometry was performed on a Varian LC-MS 500 (50−2000 Da) using isopropanol/ethyl acetate as solvent. GPC was performed using a PolymerLaboratoriesGPC50 Plus chromatograph at 35 °C with THF as elutant at a flow rate of 1.0 mL min^{-1}. Polystyrene standards were used for calibration. UV−vis spectra were recorded on a Varian 50 Scan UV−visible spectrophotometer in dichloromethane or tetrahydrofuran solution. Differential scanning calorimetry (DSC) measurements were performed on a TA DSC Q2000 in a temperature range from −50 to 150 °C in three cycles with a heating rate of 10 °C min^{-1}. Elemental analyses were performed by the microanalytic laboratory of the Department of Inorganic Chemistry at the Technical University of Munich.

General Procedure for Preparation of Aldehydes.[30] *p*-Hydroxybenzaldehyde (1 equiv) and K_2CO_3 (3.2 equiv) were added as solids to 100 mL of Ar-purged DMF (*ca.* 100 mL) at room temperature. The required bromoalkane (^{n}PrBr or ^{i}PrBr, 3.5 equiv) was added via syringe, a reflux condenser was fitted to the reaction vessel, and the resulting mixture was heated to 55 °C. When the starting material could no longer be observed by TLC analysis, water was added to dissolve the solid precipitate. The product was extracted with EtOAc (4 × 50 mL) and the organic fractions combined, washed with water (4 × 50 mL) and base washed with NaOH (aqueous 10%, 50 mL) to remove traces of unreacted *p*-hydroxybenzaldehyde. The pale yellow organic phase was separated, dried over $MgSO_4$ and all volatiles removed *in vacuo*. The resulting off-white liquid was purified by column chromatography (SiO_2, 2:1 light petroleum ether:diethyl ether) to afford a colorless liquid.

*p-n-Propoxybenzaldehyde (**1d**).* *p*-hydroxybenzaldehyde, 10.0 g, 8.19 × 10^{-2} mol; *n*-propyl bromide, 26.1 mL, 0.29 mol; K_2CO_3, 36.2 g, 0.26 mol. Yield: 11.4 g, 85%. ^{1}H NMR ($CDCl_3$, 300.1 MHz) δ 0.98 (t, $^3J_{HH}$ = 8.0 Hz, 3H, $OCH_2CH_2CH_3$), 1.76 (sext, $^3J_{HH}$ = 8.0 Hz, 2H, $OCH_2CH_2CH_3$), 3.92 (t, $^3J_{HH}$ = 8.0 Hz, 2H, $OCH_2CH_2CH_3$), 6.92 (d, $^3J_{HH}$ = 9.0 Hz, 2H, Ar*H*), 7.74 (d, $^3J_{HH}$ = 9.0 Hz, 2H, Ar*H*), 9.80 (s, 1H, ArC*H*O). ^{13}C{^{1}H} NMR ($CDCl_3$, 75.5 MHz) δ 10.4 (s, $OCH_2CH_2CH_3$), 22.4 (s, $OCH_2CH_2CH_3$), 69.8 (s, $OCH_2CH_2CH_3$), 144.7 (s, Ar*C*), 129.7 (s, Ar*C*), 131.9 (s, Ar*C*), 164.2 (s, Ar*C*), 190.6 (s, ArCHO). MS (ESI$^+$): m/z = 165.1 [M + H]$^+$; 123.1 [M − Pr + H]$^+$.

*p-Isopropoxybenzaldehyde (**1e**).* *p*-Hydroxybenzaldehyde, 10.04 g, 8.22 × 10^{-2} mol; isopropyl bromide, 27.0 mL, 0.29 mol; K_2CO_3, 36.5 g, 0.26 mol. Yield: 12.3 g, 91%. ^{1}H NMR ($CDCl_3$, 300.1 MHz) δ 1.35 (d, $^3J_{HH}$ = 6.0 Hz, 6H, $OCH(CH_3)_2$), 4.64 (sept, $^3J_{HH}$ = 6.0 Hz, 1H, $OCH(CH_3)_2$), 6.93 (d, $^3J_{HH}$ = 9.0 Hz, 2H, Ar*H*), 7.79 (d, $^3J_{HH}$ = 9.0 Hz, 2H, Ar*H*), 9.84 (s, 1H, ArC*H*O). ^{13}C{^{1}H} ($CDCl_3$, 75.5 MHz) δ 21.9 (s, $OCH(CH_3)_2$), 70.3 (s, $OCH(CH_3)_2$), 115.6 (s, Ar*C*), 129.6 (s, Ar*C*), 132.1 (Ar*C*), 163.2 (Ar*C*), 190.8 (s, ArCHO). MS (ESI$^+$): m/z = 123.0 [M − Pr + H]$^+$.

General Procedure for Porphyrin Preparation. Porphyrin synthesis was performed according to an appropriate variation of a literature

dx.doi.org/10.1021/ma301205g | *Macromolecules* 2012, 45, 6840−6849

procedure.[31] Under air, a three-neck 500 mL round-bottom flask fitted with two pressure-equalizing dropping funnels was charged with propionic acid (300 mL). Equimolar equivalents of freshly distilled pyrrole and the appropriately substituted benzaldehyde were added via syringe into the two dropping funnels, respectively, and the main reaction vessel heated to 140 °C. The contents of the dropping funnels were added to the refluxing acid dropwise over the course of 0.25 h and the resulting mixture allowed to reflux for a further 2 h. Upon cooling of the mixture to room temperature, the mixture was filtered affording a purple crystalline solid. This precipitate was washed sequentially with water (*ca.* 20 mL) and a minimum of cold methanol (*ca.* 10 mL) and allowed to dry under air. The solid was recrystallized twice from $CHCl_3$/MeOH to afford a bright purple crystalline solid.

5,10,15,20-Tetraphenyl-21H,23H-porphyrin (**2a**). Benzaldehyde, 14.0 mL, 0.14 mol; pyrrole, 9.5 mL, 0.14 mol. Yield: 3.39 g, 16%. ^{1}H NMR ($CDCl_3$, 300.1 MHz) δ −2.73 (s, 2H, N*H*), 7.74−7.80 (m, 12H, Ph*H*), 8.12−8.28 (m, 8H, Ph*H*), 8.88 (s, 8H, β-porph*H*). ^{13}C{^{1}H} NMR ($CDCl_3$, 75.5 MHz) δ 120.3 (s, Ar*C*), 126.8 (s, Ar*C*), 127.9 (s, Ar*C*), 131.0 (s, β-porph*C*), 134.7 (s, Ar*C*), 142.3 (*meso*-porph*C*) [α-porphyrin carbon not observed]. MS (ESI$^+$): m/z = 615.1 [M]$^+$, 636.9 [M + Na]$^+$. UV−vis (nm): 415.0, 515.0, 550.0, 590.0, 650.1, Anal. Calcd for $C_{44}H_{30}N_4$: C, 85.96; H, 4.92; N, 9.12. Found: C, 85.29; H, 5.05; N, 8.99.

5,10,15,20-Tetra(p-methoxy)phenyl-21H,23H-porphyrin (**2b**). *p*-Anisaldehyde, 9.5 mL, 0.14 mol; pyrrole, 16.6 mL, 0.14 mol. Yield: 3.42 g, 14%. ^{1}H NMR ($CDCl_3$, 300.1 MHz) δ −2.75 (s, 2H, N*H*), 4.10 (s, 3H, OCH_3), 7.29 (d, $^3J_{HH}$ = 9.0 Hz, 8H, Ar*H*), 8.13 (d, $^3J_{HH}$ = 9.0 Hz, 8H, Ar*H*), 8.86 (s, 8H, β-porph*H*). ^{13}C{^{1}H} NMR (75.5 MHz): δ 55.8 (s, O*C*H$_3$), 112.3 (s, Ar*C*), 119.9 (s, Ar*C*), 131.3 (s, β-porph*C*), 134.8 (s, *meso*-porph*C*), 135.7 (s, Ar*C*), 159.5 (s, Ar*C*) [α-porphyrin carbon not observed]. MS (ESI$^+$): m/z = 734.9 [M]$^+$, 756.9 [M + Na]$^+$. UV−vis (nm): 419.9, 520.0, 554.9, 594.9, 650.1, Anal. Calcd for $C_{48}H_{38}N_4O_4$: C, 78.45; H, 5.22; N, 7.63. Found: C, 78.27; H, 5.17; N, 7.25.

5,10,15,20-Tetra(p-ethoxy)phenyl-21H,23H-porphyrin (**2c**). *p*-Ethoxybenzaldehyde, 15 mL, 0.11 mol; pyrrole, 7.5 mL, 0.11 mol. Yield: 2.75 g, 13%. ^{1}H NMR ($CDCl_3$, 300.1 MHz) δ −2.76 (s, 2H, N*H*), 1.62 (t, $^3J_{HH}$ = 6.0 Hz, 12H, OCH$_2$CH_3), 4.35 (q, $^3J_{HH}$ = 6.0 Hz, 8H, OCH_2CH$_3$), 7.29 (d, $^3J_{HH}$ = 9.0 Hz, 8H, Ar*H*), 8.11 (d, $^3J_{HH}$ = 9.0 Hz, Ar*H*), 8.86 (s, 8H, β-porph*H*). ^{13}C{^{1}H} NMR (75.5 MHz): δ 15.2 (s, OCH$_2$CH$_3$), 63.9 (s, OCH$_2$CH$_3$), 112.8 (s, Ar*C*), 114.6 (s, Ar*C*), 127.7 (s, β-porph*C*), 134.7 (s, *meso*-porph*C*), 135.8 (s, Ar*C*), 146.5 (s, α-porph*C*), 158.9 (s, Ar*C*). MS (ESI$^+$): m/z = 791.0 [M]$^+$, 812.8 [M + Na]$^+$. UV−vis (nm): 419.9, 520.0, 554.9, 594.9, 650.1, Anal. Calcd for $C_{52}H_{46}N_4O_4$: C, 78.96; H, 5.87; N, 7.08. Found: C, 78.28; H, 6.05; N, 6.82.

5,10,15,20-Tetra(p-n-propoxy)phenyl-21H,23H-porphyrin (**2d**). *p*-*n*-Propoxybenzaldehyde, 12.5 g, 7.61 × 10^{-2} mol; pyrrole, 5.3 mL, 7.61 × 10^{-2} mol. Yield: 2.86 g, 12%. ^{1}H NMR ($CDCl_3$, 300.1 MHz) δ −2.74 (s, 2H, N*H*), 1.21 (t, $^3J_{HH}$ = 7.5 Hz, 12H, OCH$_2$CH$_2$CH_3), 2.02 (sext, $^3J_{HH}$ = 7.5 Hz, 8H, OCH$_2$CH_2CH$_3$), 4.22 (t, $^3J_{HH}$ = 7.5 Hz, 8H, OCH_2CH$_2$CH$_3$), 7.28 (d, $^3J_{HH}$ = 9.0 Hz, 8H, Ar*H*), 8.12 (d, $^3J_{HH}$ = 9.0 Hz, 8H, Ar*H*), 8.87 (s, 8H, β-porph*H*). ^{13}C{^{1}H} NMR ($CDCl_3$, 75.5 MHz) δ 11.0 (s, OCH$_2$CH$_2$CH$_3$), 23.0 (s, OCH$_2$CH$_2$CH$_3$), 70.0 (s, OCH$_2$CH$_2$CH$_3$), 112.8 (s, Ar*C*), 120.0 (s, Ar*C*), 131.0 (s, β-porph*C*), 134.6 (s, *meso*-porph*C*), 135.7 (s, Ar*C*), 159.0 (s, Ar*C*), [α-porphyrin carbon not observed]. MS (ESI$^+$): m/z = 847.0 [M]$^+$, 868.8 [M + Na]$^+$. UV−vis (nm): 419.9, 520.0, 554.9, 594.9, 650.1, Anal. Calcd for $C_{56}H_{54}N_4O_4$: C, 79.39; H, 6.44; N, 6.62. Found: C, 78.89; H, 6.48; N, 6.46.

5,10,15,20-Tetra(p-isopropoxy)phenyl-21H,23H-porphyrin (**2e**). *p*-Isopropoxybenzaldehyde, 13.5 g, 8.22 × 10^{-2} mol; pyrrole, 5.7 mL, 8.22 × 10^{-2} mol. Yield: 4.22 g, 24%. ^{1}H NMR ($CDCl_3$, 300.1 MHz) δ −2.72 (s, 2H, N*H*), 1.57 (d, $^3J_{HH}$ = 6.0 Hz, 24H, OCH(CH_3)$_2$), 4.86 (sept, $^3J_{HH}$ = 6.0 Hz, 4H, OC*H*(CH$_3$)$_2$), 7.27 (d, $^3J_{HH}$ = 9.0 Hz, 8H, Ar*H*), 8.12 (d, $^3J_{HH}$ = 9.0 Hz, 8H, Ar*H*), 8.90 (s, 8H, β-porph*H*). ^{13}C{^{1}H} NMR ($CDCl_3$, 75.5 MHz) δ 22.5 (s, OCH(*C*H$_3$)$_2$), 70.3 (s, O*C*H(CH$_3$)$_2$), 114.0 (s, Ar*C*), 120.0 (s, Ar*C*), 131.0 (s, β-porph*C*), 134.5 (s, *meso*-porph*C*), 135.9 (s, Ar*C*), 157.8 (s, Ar*C*), [α-porphyrin carbon not observed]. MS (ESI$^+$): m/z = 846.9 [M]$^+$, 868.9 [M + Na]$^+$. UV−vis (nm): 419.9, 520.0, 554.9, 594.9, 650.1, Anal. Calcd for $C_{56}H_{54}N_4O_4$: C, 79.39; H, 6.44; N, 6.62. Found: C, 79.25; H, 6.65; N, 6.53.

Synthesis of 5,10,15,20-Tetra(nitro)phenyl-21H,23H-porphyrin (**2f**).[32] Under air, a solution of 4-nitrobenzaldehyde (4.0 g, 2.6 × 10^{-2} mol) and acetic anhydride (2 mL) in propionic acid (100 mL) was heated to 100 °C. Pyrrole (1.85 mL, 2.6 × 10^{-2} mol) was added dropwise to the hot solution and the mixture was maintained at 100 °C for a further hour. The resulting solution was allowed to cool and stand in air for 18 h. Filtration of the tar-like mixture afforded a black solid which was washed with water (5 × 50 mL) and dried *in vacuo*. The residue was taken into pyridine (50 mL) and heated to 120 °C for 1 h. The resulting mixture was hot filtered to remove any residual solid and the pyridine removed under vacuum. Soxhlet extraction of the black solid with acetone afforded a purple solid (1.0 g, 19%).

^{1}H NMR ($CDCl_3$/DMSO-d_6) δ 0.02 (s, 2H, N*H*), 8.59 (s, 8H, β-porph*H*), 8.84 (d, $^3J_{HH}$ = 9 Hz, 8H, ArH), 8.87 (d, $^3J_{HH}$ = 9 Hz, 8H, ArH). MS (ESI$^+$): m/z = 794.8 [M]$^+$. UV−vis (nm): 427.9, 516.0, 552.0, 592.0, 646.0. Anal. Calcd for $C_{44}H_{26}N_8O_8$: C, 66.50; H, 3.50; N, 14.10. Found: C, 65.81; H, 3.30; N, 13.95.

[The limited solubility of **2f** in $CDCl_3$/DMSO precluded further purification and study by ^{13}C{^{1}H} NMR spectroscopy.]

General Procedure for Porphyrin Complexation/Oxidation. Porphyrin Complexation with Co(OAc)$_2$. A 100 mL three neck round-bottom flask was charged with DMF (*ca.* 50 mL) and the solvent degassed with Ar for 5 min. The porphyrin (1.0 equiv) was added to the main reaction vessel as a solid, a reflux condenser fitted and the mixture heated to 110 °C. Anhydrous Co(OAc)$_2$ (1.5 equiv) was then added to the mixture as a solid under a flow of Ar and the mixture allowed to stir at 110 °C for a further 1 h until TLC analysis (SiO_2, $CHCl_3$ elutant) showed no trace of free porphyrin. The resulting mixture was cooled to 0 °C and quenched by the addition of ice−water. The purple precipitate was collected by filtration, washed with water and allowed to dry in air. The obtained material was used in the subsequent oxidation without further purification.

Oxidation of [Porphyrin−Co^{II}] to [Porphyrin−Co^{III}Cl]. Under air, a methanolic solution (ca. 40 mL of MeOH) of the [porphyrin−Co^{II}] complex was treated with HCl (37%, aq.) and the resulting mixture allowed to stir at 50 °C until the formation of a precipitate was noted and the [porphyrin−Co^{II}] complex could not be detected by UV−visible spectroscopy or TLC analysis (SiO_2, $CHCl_3$ elutant). The precipitates were collected by filtration, washed with a minimum of cold methanol and thoroughly dried *in vacuo*. The obtained solids were recrystallized twice from CH_2Cl_2/pentane affording bright purple crystalline solids.

[5,10,15,20-Tetraphenylporphyrin]cobalt(II) (**3a**). 5,10,15,20-Tetraphenyl-21*H*,23*H*-porphyrin, 3.38 g, 5.50 × 10^{-3} mol; Co(OAc)$_2$, 1.46 g, 8.25 × 10^{-3} mol. Yield: 3.40 g, 92%. MS: ESI$^+$ m/z = 671.0 [M]$^+$, 687.9 [M−OH]$^+$, 710.9 [M−OH+Na]$^+$. UV−vis (nm) (THF solution): 415.0, 515.0/550.0, 589.0, 650.9.

[5,10,15,20-Tetraphenylporphyrin]cobalt(III) Chloride (**4a**). [5,10,15,20-Tetraphenylporphyrin]cobalt(II), 2.15 g, 3.20 × 10^{-3} mol; HCl (2 mL). Yield: 2.04 g, 90%. ^{1}H NMR ($CDCl_3$, 300.1 MHz); δ 7.93−8.08 (m, 12H, Ar*H*), 8.56−8.67 (m, 16H, β-porph*H* + Ar*H*). ^{13}C{^{1}H} NMR ($CDCl_3$, 75.5 MHz) δ 122.7 (s, Ar*C*), 128.1 (s, Ar*C*), 128.5 (s, Ar*C*), 130.1 (s, α-porph*C*), 139.1 (s, Ar*C*), 140.0 (s, β-porph*C*), 146.1 (s, *meso*-porph*C*). MS: ESI$^+$ m/z = 670.9 [M − Cl]$^+$. UV−vis (nm) (CH_2Cl_2 solution): 445.0, 664.9. FT-IR (ATR): 3412 w, 2958 w, 2871 w, 1485 m, 1439 m, 1230 m, 1176 m, 1071 m, 1001 m, 979 m, 841 m, 802 s, 762 m, 704 s. Anal. Calcd for $C_{44}H_{28}N_4CoCl$: C, 74.73; H, 4.00, N; 7.92. Calcd for $C_{44}H_{28}N_4CoCl + H_2O$: C, 72.87; H, 4.18; N, 7.72. Found: C, 73.25; H, 4.38; N, 7.58.

[5,10,15,20-Tetra(p-methoxy)phenylporphyrin]cobalt(II) (**3b**). 5,10,15,20-Tetra(*p*-methoxy)phenyl-21*H*,23*H*-porphyrin, 1.47 g, 2.00 × 10^{-3} mol; Co(OAc)$_2$, 0.532 g, 3.01 × 10^{-3} mol. Yield: 1.36 g, 86%. MS: ESI$^+$ m/z = 791.0 [M]$^+$, 807.8 [M − OH]$^+$, 830.8 [M − OH + Na]$^+$. UV−vis (nm) (THF solution): 419.9, 518.0/550.0, 596.0, 652.0.

[5,10,15,20-Tetra(p-methoxy)phenylporphyrin]cobalt(III) Chloride (**4b**). 5,10,15,20-Tetra(*p*-methoxy)phenylporphyrin cobalt(II), 1.20 g, 1.52 × 10^{-3} mol; HCl (2 mL). Yield: 1.17 g, 93%. ^{1}H NMR

Scheme 1. Synthesis of Porphyrin−Cobalt(III) Chloride Complexes 4a−f

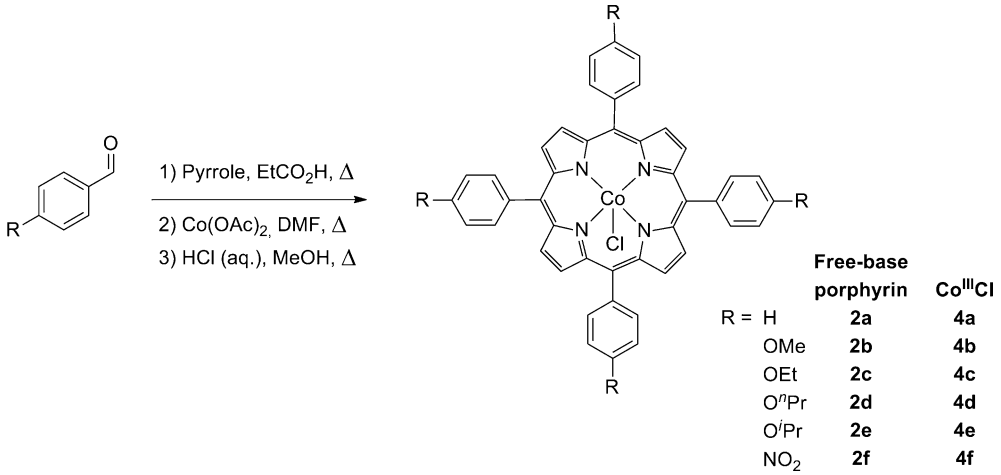

($CDCl_3$, 300.1 MHz) δ 4.16 (s, 12H, OCH_3), 7.53 (d, 8H, $^3J_{HH}$ = 9.0 Hz, Ar*H*), 8.46−8.64 (m, 16H, Ar*H* + β-porph*H*). $^{13}C\{^1H\}$ NMR ($CDCl_3$, 75.5 MHz) δ 56.0 (s, OCH_3), 114.2 (s, Ar*C*), 127.9 (s, Ar*C*), 133.5 (s, Ar*C*), 140.5 (s, β-porph*C*), 146.4 (s, *meso*-porph*C*), 161.6 (s, Ar*C*) [α-porphyrin carbon not observed]. MS: ESI^+ m/z = 791.0 [M-Cl]$^+$. UV−vis (nm) (CH_2Cl_2 solution): 453.0, 691.1. FT-IR (ATR): 3429 w, 3357 w, 2959 w, 2833 w, 1597 m, 1506 m, 1483 m, 1349 m, 1292 m, 1235 s, 1174 s, 1010 m, 984 m, 803 s, 724 m, Anal. Calcd for $C_{48}H_{36}N_4O_4CoCl$: C, 69.69; H, 4.40, N, 6.77; Calcd for $C_{48}H_{36}N_4O_4CoCl + H_2O$: C, 68.20; H, 4.54; N, 6.63. Found: C, 67.67; H, 4.49; N, 6.48.

[5,10,15,20-Tetra(p-ethoxy)phenylporphyrin]cobalt(II) (**3c**). 5,10,15,20-Tetra(*p*-ethoxy)-phenyl-21*H*,23*H*-porphyrin, 1.50 g, 1.90 × 10^{-3} mol; $Co(OAc)_2$, 0.50 g, 2.85 g × 10^{-3} mol. Yield: 1.47 g, 91%. MS: ESI^+ m/z = 847.0 [M]$^+$, 863.8 [M−OH]$^+$. UV−vis (nm) (THF solution): 417.9, 540.0/550.0, 598.9, 653.0.

[5,10,15,20-Tetra(p-ethoxy)phenylporphyrin]cobalt(III) Chloride (**4c**). 5,10,15,20-Tetra(*p*-ethoxy)phenylporphyrin cobalt(II), 1.20 g, 1.42 × 10^{-3} mol; HCl (2 mL). Yield: 1.11 g, 89%. ^1H NMR ($CDCl_3$, 300.1 MHz) δ 1.66 (t, $^3J_{HH}$ = 6.0 Hz, 12H, OCH_2CH_3), 4.40 (q, $^3J_{HH}$ = 6.0 Hz, 8H, OCH_2CH_3), 7.52 (d, $^3J_{HH}$ = 9.0 Hz, 8H, Ar*H*), 8.43−8.58 (m, 16H, β-porph*H* + Ar*H*). $^{13}C\{^1H\}$ NMR ($CDCl_3$, 75.5 MHz) δ 15.1 (s, OCH_2CH_3), 64.2 (s, OCH_2CH_3), 114.6 (s, Ar*C*), 127.9 (s, Ar*C*), 133.3 (s, Ar*C*), 140.4 (s, β-porph*C*), 146.4 (s, *meso*-porph*C*), 161.1 (s, Ar*C*) [α-porphyrin carbon not observed]. MS: ESI^+ m/z = 846.9 [M-Cl]$^+$. UV−vis (nm) (CH_2Cl_2 solution): 455.0, 692.9. FT-IR (ATR): 3426 w, 2972 w, 2869 w, 1594 m, 1482 m, 1292 m, 1231 s, 1174 s, 1035 m, 819 s, 795 s, 693 m, Anal. Calcd for $C_{52}H_{44}N_4O_4CoCl$: C, 70.70; H, 5.03; N. 6.34. Calcd for $C_{52}H_{44}N_4O_4CoCl + H_2O$: C, 69.29; H, 5.15; N, 6.22. Found: C, 67.87; H, 5.15; N, 5.93.

[5,10,15,20-Tetra(p-n-propoxy)phenylporphyrin]cobalt(II) (**3d**). 5,10,15,20-Tetra(*p*-*n*-propoxy)-phenyl-21*H*,23*H*-porphyrin, 2.02 g, 2.39 × 10^{-3} mol; $Co(OAc)_2$, 0.63 g, 3.58 × 10^{-3} mol. Yield: 1.59 g, 74%. MS: ESI^+ m/z = 903.0 [M]$^+$, 919.9 [M − OH]$^+$. UV−vis (nm) (THF solution): 417.9, 530.0, 606.1, 669.0.

[5,10,15,20-Tetra(p-n-propoxy)phenylporphyrin]cobalt(III) Chloride (**4d**). [5,10,15,20-Tetra(*p*-*n*-propoxy)phenylporphyrin]cobalt(II), 1.35 g, 1.49 × 10^{-3} mol; HCl (2 mL). Yield: 1.21 g, 86%. ^1H NMR (300.1 MHz, $CDCl_3$) δ 1.19 (t, $^3J_{HH}$ = 6.0 Hz, 12H, $OCH_2CH_2CH_3$), 1.99 (sext., $^3J_{HH}$ = 6.0 Hz, 8H, $OCH_2CH_2CH_3$), 4.20 (t, $^3J_{HH}$ = 6.0 Hz, 8H $OCH_2CH_2CH_3$), 7.23 (m, [solvent overlap], Ar*H*), 8.06 (d, $^3J_{HH}$ = 6.0 Hz, 8H, Ar*H*), 9.05 (s, 8H, β-porph*H*). $^{13}C\{^1H\}$ NMR (75.5 MHz, $CDCl_3$/DMSO-d_6) δ 10.8 (s, $OCH_2CH_2CH_3$), 22.9 (s, $OCH_2CH_2CH_3$), 69.8 (s, $OCH_2CH_2CH_3$), 112.9 (s, Ar*C*), 134.2 (s, Ar*C*), 135.4 (s, β-porph*C*), 142.0 (s, Ar*C*), 144.8 (s, *meso*-porph*C*), 159.0 (s, Ar*C*) [α-porphyrin carbon not observed]. MS: ESI^+ m/z = 903.0 [M-Cl]$^+$. UV−vis (nm) (CH_2Cl_2 solution): 428.0, 545.0. FT-IR (ATR): 3414 w, 2960 w, 2873 w, 1603 m, 1501 m, 1466 m, 1241 m, 1173 s, 1108 m, 964 m, 800 s, 737 m, Anal. Calcd for $C_{56}H_{52}N_4O_4CoCl$: C, 70.24; H, 5.70; N, 5.85. Calcd for $C_{56}H_{52}N_4O_4CoCl + H_2O$: C, 71.59; H, 5.59; N, 5.97. Found: C, 69.77; H, 5.90; N, 5.46.

[5,10,15,20-tetra(p-isopropoxy)phenylporphyrin]cobalt(II) (**3e**). [5,10,15,20-Tetra(*p*-isopropoxy)phenyl-21*H*,23*H*-porphyrin, 2.28 g, 2.69 × 10^{-3} mol; $Co(OAc)_2$, 0.71 g, 4.03 × 10^{-3} mol. Yield: 2.01 g, 83%. MS: ESI^+ m/z = 903.0 [M]$^+$, 919.9 [M−OH]$^+$. UV−vis (nm) (THF solution): 419.0, 528.0, 602.1, 653.0.

[5,10,15,20-tetra(p-isopropoxy)phenylporphyrin]cobalt(III) Chloride (**4e**). [5,10,15,20-Tetra(*p*-isopropoxy)phenylporphyrin]cobalt(II), 1.67 g, 1.85 × 10^{-3} mol; HCl, 2 mL. Yield: 1.63 g, 94%. ^1H NMR (300.1 MHz, $CDCl_3$) δ 1.57 (d, $^3J_{HH}$ = 6.0 Hz, 24H, $OCH(CH_3)_2$), 4.86 (sept. $^3J_{HH}$ = 6.0 Hz, 4H, $OCH(CH_3)_2$), 7.73 (m [solvent overlap], Ar*H*), 8.08 (d, $^3J_{HH}$ = 9.0 Hz, 8H, Ar*H*), 9.06 (s, 8H, β-porph*H*). $^{13}C\{^1H\}$ NMR (75.5 MHz, $CDCl_3$/DMSO-d_6) δ 22.4 (s, $OCH(CH_3)_2$), 70.2 (s, $OCH(CH_3)_2$), 114.1 (s, Ar*C*), 120.4 (s, α-porph*C*), 134.2 (s, Ar*C*), 135.3 (s, β-porph*C*), 144.0 (s, Ar*C*), 144.9 (s, *meso*-porph*C*), 157.8 (s, Ar*C*). MS: ESI^+ m/z = 903.2 [M − Cl]$^+$. UV−vis (nm) (CH_2Cl_2 solution): 429.0, 546.1. FT-IR (ATR): 3480 w, 2973 w, 2905 w, 1605 m, 1501 s, 1349 m, 1281 m, 1243 s, 1182 m, 1103 m, 1101 m, 950 m, 798 s, 713 m, Anal. Calcd for $C_{56}H_{52}N_4O_4CoCl$: C, 70.24; H, 5.70; N, 5.85. Calcd for $C_{56}H_{52}N_4O_4CoCl + H_2O$: C, 71.59; H, 5.59; N, 5.97. Found: C, 70.78; H, 5.98; N, 5.61.

[5,10,15,20-Tetra(p-nitro)phenylporphyrin]cobalt(II) (**3f**). 5,10,15,20-Tetra(*p*-nitro)phenylporphyrin (**2f**), 0.21 g, 2.64 × 10^{-4} mol; $Co(OAc)_2$, 0.07 g, 3.96 × 10^{-4} mol. Yield: 0.18 g, 81%. MS: ESI^+ m/z = 850.8 [M^{II}]$^+$. UV−vis (nm) (THF solution): 422.0, 516.1, 591.9, 646.9.

[5,10,15,20-Tetra(p-nitro)phenylporphyrin]cobalt(III) (**4f**). [5,10,15,20-Tetra(*p*-nitro)phenylporphyrin]cobalt(II) (**3f**), 0.11 g, 1.29 × 10^{-4} mol; HCl, 0.5 mL. Yield: 0.096 g, 84%. ^1H NMR ($CDCl_3$/DMSO-d_6): δ 8.35 (d, $^3J_{HH}$ = 6 Hz, Ar*H*), 8.60 (d, $^3J_{HH}$ = 6 Hz, ArH), 8.98 (s, 8H, β-porph*H*). $^{13}C\{^1H\}$ ($CDCl_3$/DMSO-d_6): δ 118.1 (s, α-porph*C*), 122.1 (s, Ar*C*), 134.5 (s, Ar*C*), 134.9 (s, β-porph*C*), 143.5 (s, *meso*-porph*C*), 147.9 (s, Ar*C*), 148.1 (s, Ar*C*). MS (ESI^+): m/z = 850.4 [M−Cl]$^+$. UV−vis (nm) (CH_2Cl_2 solution): 454.9, 664.0; CHN: FT-IR (ATR): 3492 w, 2941 w, 2862 w, 1596 m, 1489 s, 1338 s, 1234 m, 1107 m, 1002 m, 979 m, 864 m, 817 s, 771 m, 749 m, 709 s. Calcd for $C_{44}H_{24}N_8O_8CoCl$: C, 59.57; H, 2.73; N, 12.63. Calcd for $C_{44}H_{24}N_8O_8CoCl + H_2O$: C, 58.39; H, 2.90; N, 12.38. Found: C, 58.13; H, 3.37; N, 12.23.

Polymerization Procedure. *General Procedure for Propylene Oxide Homopolymerizations.* Under Ar, a 50 mL Schlenk flask was charged with a porphyrin catalyst (0.06 mol %) and the PPNCl cocatalyst (0.06 mol %) if required. Two mL PO (2.86 × 10^{-2} mol) was added to the reaction vessel via syringe and the resulting mixture allowed to stir for 18 h at 25 °C. A small aliquot was then removed for

dx.doi.org/10.1021/ma301205g | *Macromolecules* 2012, 45, 6840−6849

analysis by ^{1}H NMR spectroscopy. Because of the low conversions, the formed polymer was not isolated.

General Procedure for Propylene Oxide/Carbon Dioxide Copolymerizations. The required catalyst (0.05 mol %) together with an equimolar amount of PPNCl cocatalyst was added to a dry 250 mL stainless steel autoclave and propylene oxide (5 mL, 7.15×10^{-2} mol)/CH_2Cl_2 (5 mL) were added via syringe under a stream of argon. The autoclave was then pressurized with CO_2 and heated to the required temperature in an oil bath, if required. The reaction was terminated after 18 h by cooling the reactor to 0 °C and slow release of pressure. A small aliquot of the copolymerization mixture was removed for analysis by ^{1}H NMR spectroscopy and the resulting mixture dissolved in CH_2Cl_2. The crude reaction mixture was poured into methanolic HCl solution (0.5 mol dm^{-3}) and the polymer precipitated by addition of excess methanol. Residual co-containing impurities were removed from the precipitated polymer by heating a $CHCl_3$ solution of the polymer to reflux with activated charcoal followed by hot filtration of the colorless solution. After evaporation of the solvent, the poly(propylene carbonate) was dried in a vacuum oven to constant weight.

RESULTS AND DISCUSSION

Synthesis of Complexes. The free porphyrins **2a−f** were synthesized by variations of acid-catalyzed Rothemund procedures with pyrrole and an appropriately substituted benzaldehyde, Scheme 1.[30−32] To establish the effect of ligand substitution on the complex activity, the unsubstituted tetraphenylporphyrin (**2a**) was also prepared. Formation of the Co^{III}Cl porphyrin complexes **4a−f** was easily achieved in a two-step procedure via complexation with $Co(OAc)_2$ and subsequent oxidation of the metal center in methanolic HCl solution at 50 °C.

The NMR spectra of the air stable diamagnetic porphyrin Co(III) complexes were largely similar to those of the parent free-base porphyrins **2a−e** with only moderate shifts of the resonances attributed to the β-porphyrin protons observed.[33] CHN microanalyses of the oxidized Co(III) complexes **4a−f** corresponded to the incorporation of one molecule of water per metal center which could not be removed by drying of the complexes under high vacuum. The presence of this coordinated water was confirmed by both the appearance of absorption bands in the region 3300−3500 in their IR spectra[34] and resonances corresponding to H_2O by ^{1}H NMR spectroscopy (Supporting Information, S47).

Propylene Oxide Homopolymerization of Catalysts 4a−e. To establish the reactivity of the substituted complexes **4b−f** as catalysts in epoxide ring-opening homopolymerization experiments with propylene oxide (PO) were performed. Consistent with previous observations,[35] the unsubstituted cobaltoporphyrin **4a** showed no activity toward PO polymerization, even in the presence of PPNCl cocatalyst. By contrast, complexes **4b−e**/PPNCl systems show low reactivity toward the formation of poly(propylene oxide) (PPO) with small TON/TOF numbers, Table 1. Experiments with the nitro-substituted complex **4f** showed no activity toward PO ring-opening, even in the presence of PPNCl additive. These results lead to the conclusion that the activity of the central cobalt ion toward epoxide ring-opening is significantly influenced by the electronic environment of the porphyrin as the incorporation of electronically differing substituents into the periphery of the ligand framework clearly modulates the overall binding environment at the metal center. Previous studies of unsubstituted 5,10,15,20-tetraphenylporphyrin (TPP) M(III)$^+$ complexes by Chisholm and co-workers have indicated that the (TPP)Co$^+$ cation has a surprisingly low affinity for PO binding

Table 1. Homopolymerization of PO with Catalysts 4a−f[a]

entry	catalyst system[b]	PPO[c] (%)	TON[d]	TOF[e]/h^{-1}
1	**4a**	–	–	–
2	**4b**	2	30	2
3	**4c**	9	135	8
4	**4d**	7	105	6
5	**4e**	5	75	4
6	**4f**	–	–	–

[a]All reactions carried out in neat PO (2 mL), at 25 °C. [b][catalyst]:[PPNCl]:[PO] = 1:1:1500, 18 h reaction time. [c]Determined by ^{1}H NMR spectroscopy. [d]Moles of PO consumed per mole of Co. [e]Moles of PO consumed per mole of Co per hour.

in the gas phase (in comparison to related (TPP)Cr$^+$ and (TPP)Al$^+$ cations),[35] however, the introduction of four electron donating alkoxy- fragments clearly enhances the reactivity of the overall metal center toward epoxide binding, despite the relatively low Lewis acidity of the Co(III) ion. Indeed, porphyrin cobalt(III) complexes bearing *meso*-methoxy-substituents display catalytic activity toward α-epoxide ring-opening with a high degree of selectivity.[36] Although the alkoxy-substituted compounds **4b−e** display significantly reduced activities toward epoxide homopolymerization than related Al[37] and Cr[35] metalloporphyrins, it is noteworthy that even relatively minor modifications of the ligating porphyrin can alter the reactivity of the resulting Co complexes.

Copolymerization Behavior of Catalysts 4a-f: Effect of CO_2 Pressure. As a next step the reactivity of complexes **4a−f** toward PO/CO_2 copolymerization was explored. Experiments were initially investigated with variation of reaction pressure with a [catalyst]:[propylene oxide] ratio of 1:2000, Table 2. All copolymerization experiments were performed in the presence of a noncoordinating solvent (CH_2Cl_2) in order to reduce monomer diffusion limitations. To probe the effect of the cocatalyst on the polymerization system all metalloporphyrins were first tested for catalytic activity in the absence of the PPNCl cocatalyst. In contrast to the more Lewis acidic Al-containing porphyrins, which demonstrate moderate activity toward epoxide/CO_2 copolymerization in the absence of additives,[18,35] the Co complexes **4a−f** demonstrated no catalytic activity in this reaction.

Addition of one molar equivalent of PPNCl cocatalyst to the copolymerization reaction afforded significant reactivity of the complexes with PO/CO_2. The binary **4a−e**/PPNCl catalysts systems demonstrate high activity toward copolymerization, as reflected in their TON/TOF values, however it is striking that the **4f**/PPNCl only afforded cyclic carbonate in low yield (Table 2, entry 17). This is noteworthy in light of previous studies with Al-porphyrin binary catalyst systems where the incorporation of *meso*-fluoro substituents in the porphyrin framework afforded more active and polymer selective systems than analogous porphyrins bearing unsubstituted or β-ethyl substituents.[27] In the case of **4f** the exclusive formation of cyclic carbonate can be attributed to the electron withdrawing nature of the nitro-substituents in the catalyst framework.

The formation of cyclic carbonate is dominant in systems where the backbiting activation barriers are low enough to compete with chain propagation[38] and is known to occur by depolymerization of growing polymer chains from either the alkoxy- and carbonato- chain ends,[22] Scheme 2. In the electron-rich BDI-Zn complexes, the use of electron withdrawing groups promotes PO/CO_2 polymerization activity over cyclization by

dx.doi.org/10.1021/ma301205g | *Macromolecules* 2012, 45, 6840−6849

Table 2. Selected PO/CO_2 Copolymerization Data for 4a–f at 30 and 50 bar CO_2 Pressure

			conversion[b]									
entry	catalyst system[a]	P/bar	PPC (%)	PPO (%)	CC (%)	TON[c]	TOF[d]/h^{-1}	H–T[e] (%)	T_g[f]/°C	M_n[g] /kg mol^{-1}	PD[g]
1	**4a**	30	–	–	–	–	–	–	–	–	–
2	**4a**/PPNCl	30	50	<1	5	1112	62	93	41.5	36	1.14
3	**4a**/PPNCl	50	41	<1	5	930	52	93	40.7	33	1.38
4	**4b**	30	–	–	–	–	–	–	–	–	–
5	**4b**/PPNCl	30	68	<1	3	1420	79	93	40.7	39	1.17
6	**4b**/PPNCl	50	74	<1	3	1540	86	93	39.4	45	1.23
7	**4c**	30	-	-	-	-	-	-	-	-	-
8	**4c**/PPNCl	30	77	<1	4	1620	90	93	41.4	38	1.16
9	**4c**/PPNCl	50	74	1	3	1540	86	94	40.8	52.5	1.26
10	**4d**	30	-	-	-	-	-	-	-	-	-
11	**4d**/PPNCl	30	78	<1	2	1620	90	93	39.6	27.5	1.13
12	**4d**/PPNCl	50	73	2	3	1520	85	94	40.6	43	1.23
13	**4e**	30	–	–	–	–	–	–	–	–	–
14	**4e**/PPNCl	30	85	<1	3	1760	98	93	40.6	38	1.17
15	**4e**/PPNCl	50	81	1	3	1680	93	93	38.4	34.5	1.23
16	**4f**	30	–	–	–	–	–	–	–	–	–
17	**4f**/PPNCl	30	–	–	13	263	11	–	–	–	–

[a][catalyst]:[PO] = 1:2000/[catalyst]:[cocatalyst]:[PO] = 1:1:2000, 18 h reaction time, 25 °C. [b]Determined by ^{1}H NMR spectroscopy. [c]Moles of PO consumed per moles of Co. [d]Moles of PO consumed per mole of Co per hour. [e]Determined by $^{13}C\{^1H\}$ NMR spectral integration. [f]T_g values determined from DSC second heating cycle. [g]Determined by size exclusion chromatography using polystryrene standard.

Scheme 2. Backbiting Mechanism from Alkoxy- (A) or Carbonato- (B) Poly(carbonate) Intermediates

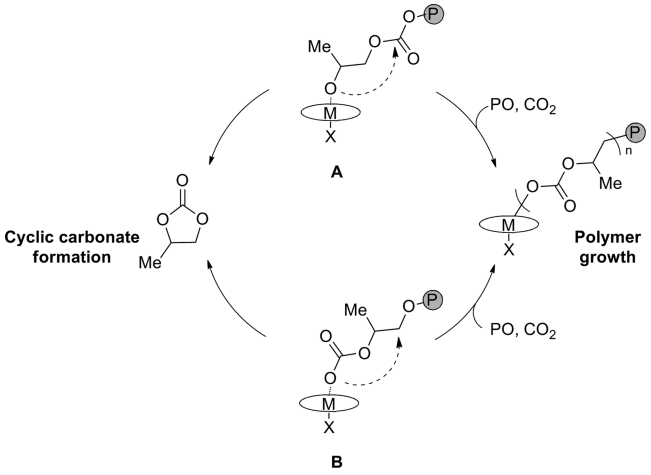

promoting epoxide insertion into the polymer chain.[39] However, it is clear in the case of **4f** that the combination of an electron poor Co^{3+} ion with a nitro-substituted ligand favors cyclization of the substrates over polymer chain propagation as a result of the electron deficient environment at the active metal site. Indeed, theoretical calculations with Zn complexes have indicated that the insertion of CO_2 into a metal-alkoxide bond has a considerably smaller energy barrier than epoxide enchainment[22] which provides further indication that the ease of epoxide incorporation into the growing polymer chain is of key importance.

For the catalyst systems capable for polymer synthesis (**4a–e**), systematic polymerization test runs with increasing CO_2 pressure allowed the determination of pressure-dependent activity profiles for each catalyst, Chart 2. Further copolymerization experiments were not undertaken with **4f** due to its propensity for cyclization. All reactions were performed with identical catalyst/cocatalyst loading to permit direct comparison and establish structure–activity patterns to be drawn. The binary **4a–e**/PPNCl systems were demonstrated to be highly active and selective copolymerization catalysts, furnishing copolymer with approaching 50% CO_2 content in high yields.

Chart 2. PPC yield (%) with Variation of CO_2 Pressure at 30 °C: 4a (Black Squares), 4b (Red Points), 4c (Green Triangles), 4d (Dark Blue Triangles), and 4e (Light Blue Rhombs)

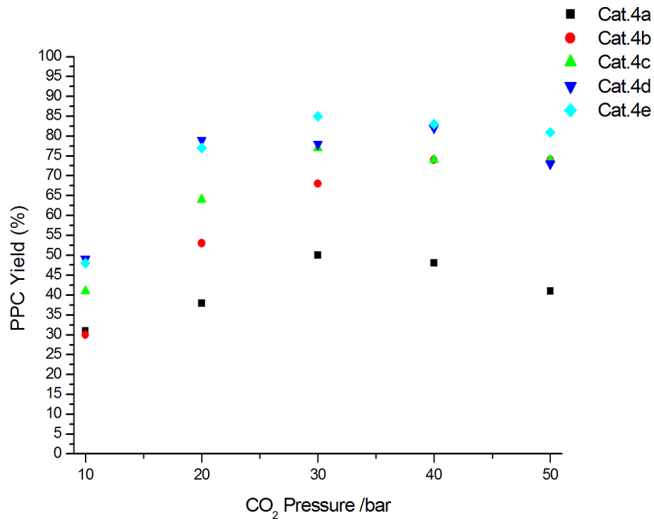

From the data in Table 2, it is readily apparent that **4b–e**, in which the porphyrin framework bears four alkoxy-fragments, displayed an overall increased PO consumption in comparison with the unsubstituted catalyst **4a**. It is clear that the inclusion of electron-donating fragments in the catalyst systems has a beneficial effect on the catalytic activity of these complexes. These substituents are presumed to have two advantageous effects on the cobaltoporphyrin systems, namely modulating both the electronic environment at the Co center and the solubility of the overall complexes. The electron donating nature of the alkoxy groups in complexes **4b–e** increases the

dx.doi.org/10.1021/ma301205g | Macromolecules 2012, 45, 6840–6849

Chart 3. Schematic Description of α-/β-Modes of Epoxide Cleavage Leading to Insertion Regioselectivity and Representative $^{13}C\{^1H\}$ NMR Spectrum Showing Resulting Polymer Regiochemistry (Carbonate Region Shown Only) (Catalyst 4b, Table 2, Entry 5, 92% H−T)

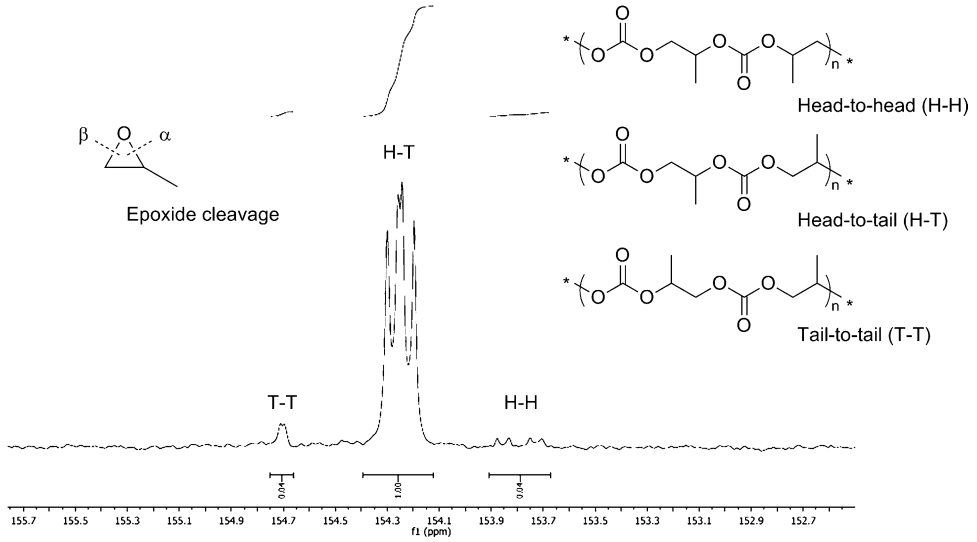

yield of copolymer in comparison to the unsubstituted **4a**. This increase in activity compares well with the observation of Darensbourg and co-workers with Cr−salen complexes in which a similar increase in catalyst activity was noted with the introduction of OMe groups to the salen−phenolate rings.[40] Furthermore, the solubility of porphyrin complexes is well-known to be influenced by substituents present at the macrocyclic framework[41] and the incorporation of four alkoxy-fragments results in an increased solubility of the metalloporphyrins in the reaction medium. Indeed, these higher activities for **4b−e** mirror studies by Inoue where the activities of Al-porphyrins substituted with methoxy groups exceeded those of unsubstituted TPPAlCl in the polymerization of PO.[29] By examination of the pressure-dependence profiles of the complexes **4b−e** (Chart 2), it is immediately apparent that the catalysts comprising the longer ethoxy (**4c**)/propoxy (**4d−e**) substituents demonstrated the highest PO consumption, as reflected in their greater TON/TOF numbers, thus indicating complex solubility in the reaction medium is of crucial importance to achieve high monomer conversions. Contrasting the PPC yield of the propoxy-substituted catalysts **4d** (78%) and **4e** (85%) at 30 bar CO_2 pressure (Table 2, Entries 11 and 14) with that of the methoxy-substituted system **4b** (Table 2, Entry 5, 68%) provides an indication of the solubility influence of the longer alkoxy-functionalities on the catalyst turnover.

By variation of reaction pressure, the optimum pressure for the copolymerization reaction for the systems **4a−e** could be determined. Chart 2 clearly shows a maximum turnover around 30 bar with a further increase in pressure having little or negative impact on the activity. The ready explanation for this observation is a dilution of the reaction mixture by the CO_2 monomer at higher pressure which causes a volumetric increase of the copolymerization medium.[42] In all copolymerization experiments, total PO consumption was not achieved due to reduced monomer diffusion in the reaction medium at higher conversions although low CC conversion (<5%) was typically observed with both the substituted and unsubstituted porphyrin systems at 30 °C.

As indicated by the low TOFs in PO homopolymerization, sequential epoxide enchainment is not favored with **4a−e** and the copolymerization of PO and CO_2 afforded almost perfectly alternating poly(carbonate) structure with minimal polyether content with moderate molecular weight (M_n). The substitution pattern of the porphyrin framework did not significantly affect the obtained polymer M_n, however GPC elugrams showed exclusively bimodal PPC character. Bimodality of poly(carbonate)s produced by porphyrin-based catalysts is regarded as a characteristic feature.[18] This attribute has been proposed to arise from the growth of poly(carbonate) chain from both sides of the rigid metalloporphyrin coordination plane,[43] however it is highly likely that the presence of water in the polymerization mixture gives rise to chain transfer reactions, which prevents exclusively monomodal polymer character. In studies with Al−porphyrin catalysts it has been suggested that the presence of adventitious water leads to complexes of reduced activity,[27] however with the air/moisture tolerant Co-porphyrins this is considered to be less likely. Elemental analysis/IR spectroscopy of **4a−e** was consistent with the presence of coordinated water to the Co center which presumably occupies an axial position of the metal's coordination sphere. Over the course of the copolymerization reaction, this water causes chain transfer reactions, resulting in these characteristic bimodal polymers. The polycarbonates obtained from the cobaltoporphyrins all exhibited narrow PD indices at 30 bar which were observed to broadened slightly upon increase in pressure to 50 bar. This further evidence a controlled, living-type polymerization mechanism in these Co-systems, thus reflecting the studies of Al-based metalloporphyrins.[44]

Independent of catalyst substitution pattern, head-to-tail (H−T) connectivity[45] in the obtained PPC, resulting from repeated α- or β-cleavage of the epoxide ring, was observed to reach 93% above 30 bar (Table 2). The comparably high degree of H−T incorporation across this series of catalysts demonstrate that the substitution of the catalyst does not influence the nature of epoxide enchainment. Indeed, the placement of the alkoxy- functionalities at the periphery of the rigidly planar porphyrin ring evidently provides a significant electronic influence to the catalytic metal center without introducing steric interference. The consistent PPC stereo-

dx.doi.org/10.1021/ma301205g | Macromolecules 2012, 45, 6840−6849

Table 3. Selected Polymerization data at 30 and 60 °C for 4a−e at 30 bar CO_2 pressure

			conversion[b]								
entry	catalyst system[a]	T/°C	PPC (%)	PPO (%)	CC (%)	TON[c]	TOF[d]/h^{-1}	H−T[e] (%)	T_g[f] /°C	M_n[g] /kg mol^{-1}	PD[g]
1	**4a/PPNCl**	30	54	<1	4	1172	65	91	41.7	41.5	1.19
2	**4a/PPNCl**	60	39	<1	22	1233	69	85	38.6	21.5	1.25
3	**4b/PPNCl**	30	68	<1	4	1440	80	91	40.8	38	1.18
4	**4b/PPNCl**	60	12	1	20	640	36	85	37.5	8	1.23
5	**4c/PPNCl**	30	85	<1	3	1760	98	92	41.1	46.5	1.20
6	**4c/PPNCl**	60	25	1	18	860	48	82	36.0	14	1.25
7	**4d/PPNCl**	30	88	<1	2	1800	100	93	40.7	47	1.18
8	**4d/PPNCl**	60	20	2	17	740	41	81	35.1	9	1.22
9	**4e/PPNCl**	30	90	<1	3	1860	103	93	38.8	39	1.18
10	**4e/PPNCl**	60	10	1	18	560	31	80	34.4	6	1.14

[a][catalyst]:[cocatalyst]:[PO] = 1:1:2000, 18 h reaction time. [b]Determined by ^{1}H NMR spectroscopy. [c]Moles of PO consumed per moles of Co. [d]Moles of PO consumed per mole of Co per hour. [e]Determined by $^{13}C\{^1H\}$ NMR spectral integration. [f]T_g values determined from DSC second heating cycle. [g]Determined by size exclusion chromatography using polystryrene standard.

chemistry indicates the inherently regioselective nature of the cobaltoporphyrin systems.

Effect of Copolymerization Temperature. A further set of experiments were performed to probe the effect of temperature on the porphyrin catalyst systems at 30 bar CO_2 pressure, Table 3. Overall an increase of reaction temperature from 30 to 60 °C resulted in a reduced PO consumption. This loss of activity was accompanied, as expected, by increased formation of cyclic carbonate as a result of the higher activation barriers for epoxide/CO_2 cyclization.[46,47] Chart 4 depicts a plot

Chart 4. Overall PO Consumption as a Function of Temperature (30 bar CO_2 Pressure): 4a (Black Squares), 4b (Red Points), 4c (Green Triangles), 4d (Dark Blue Triangles), and 4e (Light Blue Rhombs)

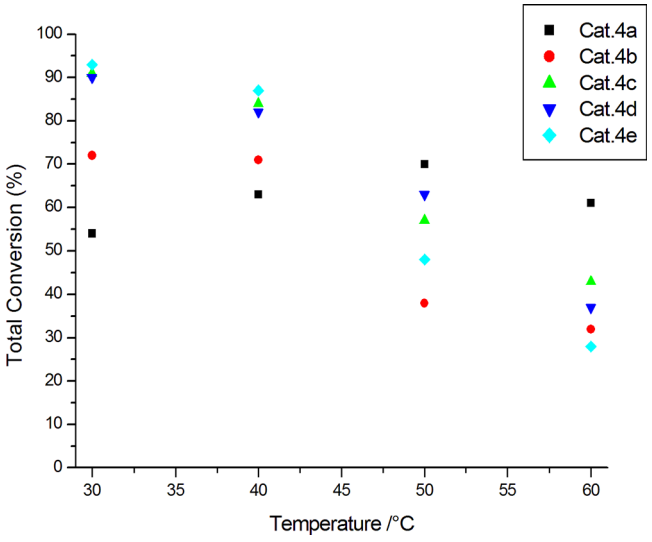

of total PO conversion as a function of increasing temperature which reveals that the unsubstituted system **4a** was least affected by a rise in reaction temperature (Chart 4, black squares) whereas the alkoxy-substituted systems exhibited dramatically reduced activity. Specifically, the activities of the higher substituted systems **4c−e** were most affected by an increase in temperature with their general PO consumption dropping from >85% at 30 °C to *ca.* 20% at 60 °C.

The overall PO consumption vs pressure can be further analyzed to demonstrate the relative product formation and therefore the selectivity of the catalyst systems with increased temperature. Chart 5 demonstrates a clear drop in PPC yield

Chart 5. PPC Yield with Variation of Temperature for 4a−e at 30 bar CO_2 Pressure; 4a (Black Squares), 4b (Red Points), 4c (Green Triangles), 4d (Dark Blue Triangles), 4e (Light Blue Rhombs)

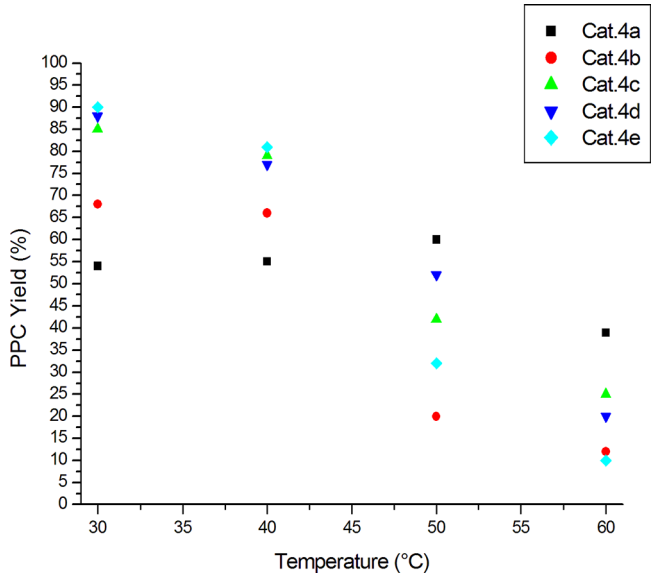

with higher reaction temperature with this being more pronounced with **4b−e**. As expected by the living catalytic nature of this process, the fall in PPC yield was accompanied by a significant reduction in polymer molecular weight, Table 3. Interestingly, the PPC obtained at higher temperature with **4a−e** remained highly alternating with only small degrees of poly(ether) linkages although a rise in polymerization temperature afforded a minor decrease in the H-T connectivity of the poly(carbonate)s. Epoxide incorporation proceeds by competitive attack at the methylene and methine ring carbons by metalloporphyrin catalysts[48] although ring-opening is favored at the least sterically hindered carbon of the ring (β-cleavage).[6,47] An increase in reaction temperature clearly leads to a greater competition between these ring-opening modes. This temperature-induced decrease of PPC regioregularity is consistent with the findings of Wang's studies with the unsubstituted **4a**/PPNCl system.[26] Associated with the reduction in the M_n of the

dx.doi.org/10.1021/ma301205g | *Macromolecules* 2012, 45, 6840−6849

PPCs was a decrease in the glass transition temperatures (T_g) of the polymers. The T_g values of poly(carbonate)s are known to be affected by the polymer chain length as well as the polymer microstructure[49] as PPC with more uniform head-to-tail character demonstrates higher T_g values than those with more regiorandom microstructures[50] which is consistent with the here presented findings.

The decrease in polymer yield was accompanied by a clear increase in cyclic carbonate formation, Chart 6. Interestingly

Chart 6. CC Yield with Variation of Temperature for 4a−e at 30 bar CO_2 Pressure: 4a (Black Squares), 4b (Red Points), 4c (Green Triangles), 4d (Dark Blue Triangles), and 4e (Light Blue Rhombs)

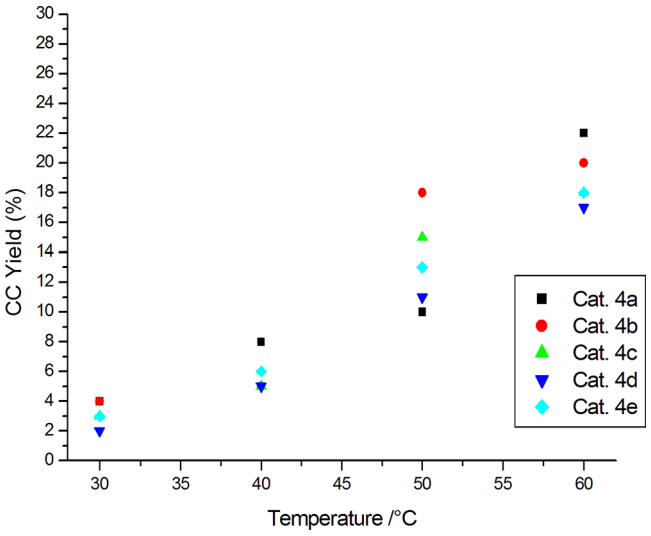

the produced amount of CC was independent of catalyst substitution pattern with a linear increase from *ca.* 4% (30 °C) to *ca.* 20% (60 °C) for all systems **4a−e**. This rise in cyclization can be broadly attributed to either an accelerated rate of depolymerization or deactivation of the cobaltoporphyrin catalysts with increased temperature. Indeed, higher reaction temperatures have been demonstrated to promote the formation of reduced Co(II) salen compounds in the copolymerization mixture,[51] a situation which may occur with the present Co(III) porphyrins as indicated by the overall fall in monomer conversion at increased temperature (Chart 4). Polymers comprising 1-alkyl-substituted epoxides are more susceptible to cyclic carbonate formation than their aromatic counterparts through chain backbiting[22,52,53] however it has previously been demonstrated that CC is capable of ligating the metal center in Zn-based systems and hindering the catalyst turnover.[38] This "self-inhibition" by side product formation would further explain the loss of activity observed with higher reaction temperatures. In addition, increase of reaction temperature may disfavor the coordination equilibrium of the epoxide to the active catalytic center and the presence of the relatively electropositive Co(III) ion is assumed to move the position of this equilibrium further to the left. The combination of these latter two effects clearly results in a reduced overall catalytic activity of the polymerization systems at elevated temperature.

CONCLUSION

Here we have presented a series of cobaltoporphyrin systems with systematically varied substitution pattern and their activities in both PO homopolymerization and PO/CO_2 copolymerization. The ease of synthesis of these rigid, symmetrical porphyrin catalysts combined with their oxygen and moisture stability presents numerous advantages over more sensitive catalyst systems.

The activity and selectivity of these cobaltoporphyrins is strongly dependent on the substitution pattern of the ligand framework and enables tailoring of the product selectivity; electron withdrawing substituents afford exclusive cyclization (forming cyclic carbonate) while electron donating fragments afford highly active copolymerization catalysts, producing poly(carbonate) with excellent properties. By placement of these electronically differing substituents at the periphery of the rigidly planar porphyrin, the electron influence of these fragments is maintained while minimizing steric clashes at the active metal site. Furthermore, our studies indicate that an increase of catalyst solubility directly impacts on the polymerization activity, as indicated by the higher turnovers for the ethoxy-/propoxy-substituted catalysts **4c−e**, which emphasizes the importance of the homogeneity of the polymerization mixture with these systems. Overall, we have demonstrated that molecular catalyst design by simple ligand modification represents a useful and underused strategy in porphyrin-based catalyst systems and has great potential to generate catalysts with high activities and tailored selectivities.

ASSOCIATED CONTENT

Supporting Information

Characterization of catalysts and precursors, representative polymer analyses and full tables of polymerization data to accompany Charts 2 and 4−6. This material is available free of charge via the Internet at http://pubs.acs.org/.

AUTHOR INFORMATION

Corresponding Author

*Telephone +49 89 289 13571. Fax +49 89 289 13562. E-mail: rieger@tum.de.

Notes

The authors declare no competing financial interest.

ACKNOWLEDGMENTS

We gratefully acknowledge the King Abdullah University of Science and Technology (KAUST), Award No. UK-C0020, KSA-C0069, for financial support. Ms. A. Jonović is thanked for technical support with TGA and GPC measurements. Mr. V. Bretzler is acknowledged for helpful comments with the preparation of this manuscript.

REFERENCES

(1) Cokoja, M.; Bruckmeier, C.; Rieger, B.; Herrmann, W. A.; Kühn, F. E. *Angew. Chem., Int. Ed.* **2011**, *50*, 8510−8537.
(2) Aresta, M.; Dibenedetto, A. *Dalton Trans.* **2007**, 2975−2992.
(3) Kember, M. R.; Buchard, A.; Williams, C. K. *Chem. Commun.* **2011**, *47*, 141−163.
(4) Darensbourg, D. J. *Chem. Rev.* **2007**, *107*, 2388−2410.
(5) Coates, G. W.; Moore, D. R. *Angew. Chem., Int. Ed.* **2004**, *43*, 6618−6639.
(6) Klaus, S.; Lehenmeier, M. W.; Anderson, C. E.; Rieger, B. *Coord. Chem. Rev.* **2011**, *255*, 1460−1479.

(7) Serini, V. In *Encyclopedia of Industrial Chemistry*, 7th ed.; Wiley-VCH Verlag GmbH & Co. KGaA: Weinheim, Germany, 2012.
(8) Koning, C.; Wildeson, J.; Parton, R.; Plum, B.; Steeman, P.; Darensbourg, D. J. *Polymer* **2001**, *42*, 3995−4004.
(9) Du, L. C.; Meng, Y. Z.; Wang, S. J.; Tjong, S. C. *J. Appl. Polym. Sci.* **2004**, *92*, 1840−1846.
(10) Takeda, N.; Inoue, S. *Makromol. Chem.* **1978**, *179*, 1377−1381.
(11) Aida, T.; Ishikawa, M.; Inoue, S. *Macromolecules* **1986**, *19*, 8−13.
(12) Ree, M.; Hwang, Y.; Kim, J.-S.; Kim, H.; Kim, G.; Kim, H. *Catal. Today* **2006**, *115*, 134−145.
(13) Gao, L. J.; Xiao, M.; Wang, S. J.; Du, F. G.; Meng, Y. Z. *J. Appl. Polym. Sci.* **2007**, *104*, 15−20.
(14) Klaus, S.; Lehenmeier, M. W.; Herdtweck, E.; Deglmann, P.; Ott, A.-K.; Rieger, B. *J. Am. Chem. Soc.* **2011**, *133*, 13151−13161.
(15) Chisholm, M. H.; Navarro-Llobet, D.; Zhao, Z. *Macromolecules* **2002**, *35*, 6494−6504.
(16) Inoue, S. *J. Polym. Sci., Part A* **2000**, *38*, 2861−2871.
(17) Riedel, E. *Moderne Anorganische Chemie*, 3rd ed.; Walter de Gruyter: Berlin, 2007; Chapter 5.
(18) Aida, T.; Inoue, S. *Acc. Chem. Res.* **1996**, *29*, 39−48.
(19) Luinstra, G. A. *Polym. Rev.* **2008**, *48*, 192−219.
(20) Lu, X.-B.; Darensbourg, D. J. *Chem. Soc. Rev.* **2012**, *41*, 1462−1484.
(21) Kuran, W.; Listoś, T. *Macromol. Chem. Phys.* **1994**, *195*, 1011−1015.
(22) Luinstra, G. A.; Haas, G. R.; Molnar, F.; Bernhart, V.; Eberhardt, R.; Rieger, B. *Chem.—Eur. J.* **2005**, *11*, 6298−6314.
(23) Sugimoto, H.; Kuroda, K. *Macromolecules* **2008**, *41*, 312−317.
(24) Paddock, R. L.; Hiyama, Y.; McKay, J. M.; Nguyen, S. T. *Tetrahedron Lett.* **2004**, *45*, 2023−2026.
(25) Jin, L.; Jing, H.; Chang, T.; Bu, X.; Wang, L.; Liu, Z. *J. Mol. Cat. A* **2007**, *261*, 262−266.
(26) Qin, Y.; Wang, X.; Zhang, S.; Zhao, X.; Wang, F. *J. Polym. Sci., Part A* **2008**, *46*, 5959−5967.
(27) Chatterjee, C.; Chisholm, M. H. *Inorg. Chem.* **2011**, *50*, 4481−4492.
(28) Sugimoto, H.; Suzuki, C.; Sasao, Y.; Ikai, S. JP2008081518A.
(29) Sugimoto, H.; Aida, T.; Inoue, S. *Macromolecules* **1990**, *23*, 2869−2875.
(30) Solladié, G.; Pasturel-Jacopé, Y.; Maignan, J. *Tetrahedron* **2003**, *59*, 3315−3321.
(31) Adler, A. D.; Longo, F. R.; Finarelli, J. D.; Goldmacher, J.; Assour, J.; Korsakoff, L. *J. Org. Chem.* **1967**, *32*, 476.
(32) Bettelheim, A.; White, B. A.; Raybuck, S. A.; Murray, R. W. *Inorg. Chem.* **1987**, *26*, 1009−1017.
(33) Abraham, R. J.; Fell, S. C. M.; Smith, K. M. *Org. Magn. Resonance* **1977**, *9*, 367−373.
(34) Socrates, G. *Infrared Characteristic Group Frequencies*, 2nd ed.; J. Wiley and Sons: Chichester, U.K., 1994.
(35) Chen, P.; Chisholm, M. H.; Gallucci, J. C.; Zhang, X.; Zhou, Z. *Inorg. Chem.* **2005**, *44*, 2588−2595.
(36) Venkatasubbaiah, K.; Zhu, X.; Kays, E.; Hardcastle, K. I.; Jones, C. W. *ACS Catalysis* **2011**, *1*, 489−492.
(37) Sugimoto, H.; Inoue, S. *Adv. Polym. Sci.* **1999**, *146*, 39−119.
(38) Lehenmeier, M. W.; Bruckmeier, C.; Klaus, S.; Dengler, J. E.; Deglmann, P.; Ott, A.-K.; Rieger, B. *Chem.—Eur. J.* **2011**, *17*, 8858−8869.
(39) Allen, S. D.; Moore, D. R.; Lobkovsky, E. B.; Coates, G. C. *J. Am. Chem. Soc.* **2002**, *124*, 14284−14285.
(40) Darensbourg, D.; Mackiewicz, R. M.; Rodgers, J. L.; Fang, C. C.; Billodeaux, D. R.; Reibenspies, J. H. *Inorg. Chem.* **2004**, *43*, 6024−6034.
(41) Mamardashvili, G. M.; Mamardashvili, N. Zh; Golubchicov, O. A.; Berezin, B. D. *J. Mol. Liq.* **2001**, *91*, 189−191.
(42) Darensbourg, D. J.; Mackiewicz, R. M.; Phelps, A. L.; Billodeaux., D. R. *Acc. Chem. Res.* **2004**, *37*, 836−844.
(43) Sugimoto, H.; Ohtsuka, H.; Inoue, S. *J. Polym. Sci., Part A* **2005**, *43*, 4172−4186.
(44) Inoue, S. *J. Polym. Sci., Part A* **2000**, *38*, 2861−2871.
(45) Assignments of $^{13}C\{^{1}H\}$ NMR spectra were made according to Lednor, P. W.; Rol, N. C. *J. Chem. Soc., Chem. Commun.* **1985**, 598−599.
(46) Darensbourg, D. J.; Yarbrough, J. C.; Ortiz, C.; Fang, C. C. *J. Am. Chem. Soc.* **2003**, *125*, 7586−7591.
(47) Darensbourg, D. J.; Andreatta, J. R.; Moncada, A. I. In *Carbon Dioxide as Chemical Feedstock*; Aresta, M., Ed.; Wiley-VCH Verlag GmbH: Weinheim, Germany, 2010, Chapter 8, pp 213−248.
(48) Chisholm, M. H.; Zhou, Z. *J. Am. Chem. Soc.* **2004**, *126*, 11030−11039.
(49) Nakano, K.; Hashimoto, S.; Nakamura, M.; Kamada, T.; Nozaki, K. *Angew. Chem., Int. Ed.* **2011**, *50*, 4868−4871.
(50) Tao, Y.; Wang, X.; Chen, X.; Zhao, X.; Wang, F. *J. Polym. Sci., Part A* **2008**, *46*, 4451−4458.
(51) Ren, W.-M.; Liu, Z.-W.; Wen, Y.-Q.; Zhang, R.; Lu, X.-B. *J. Am. Chem. Soc.* **2009**, *131*, 11509−11518.
(52) Vogdanis, L.; Martens, B.; Uchtmann, H.; Hensel, F.; Heitz, W. *Macromol. Chem.* **1990**, *191*, 465−472.
(53) Darensbourg, D. J.; Yarbrough, J. C.; Ortiz, C.; Fang, C. C. *J. Am. Chem. Soc.* **2003**, *125*, 7586−7591.